Electronic Supplementary Information (ESI)

Pyrene-based D-π-A dyes that exhibit solvatochromism and high fluorescence brightness in apolar solvents and water

Yosuke Niko,[a] Yokan Cho,[a] Susumu Kawauchi[a] Gen-ichi Konishi[a,b]

[a] Department of Organic and Polymeric Materials, Tokyo Institute of Technology, 2-12-1-H-134 O-okayama, Meguro-ku, Tokyo 152-8552, Japan., Fax: +81-3-5734-2888; Tel: +81-3-5734-2321; E-mail: konishi.g.aa@m.titech.ac.jp
[b] PRESTO, Japan Science and Technology Agency (JST).

Table of Contents

A. General Method

Instruments All the ^{1}H NMR and ^{13}C NMR spectra were recorded on a 400 MHz JEOL LMN-EX400 or 300 MHz Bruker DPX 300 instrument with tetramethylsilane (TMS) as the internal standard. FT-IR spectra were recorded on a JASCO FT-IR 469 plus spectrometer. Melting points were obtained by a Stuart Scientific Melting Point Apparatus SMP3. MS spectra (FAB) were obtained by JEOL JMS700 mass spectrometer. All photophysical measurements performed in solutions were carried out using dilute solutions with optical density (O.D.) around 0.1 at the maximum absorption wavelength in 1 cm path length quartz cells at room temperature (298 K). In addition, all samples solutions were deaerated by bubbling with argon gas for 15 min before the measurements. The UV-Vis spectra were recorded with a Beckman Coulter DU800 UV-Vis Spectrophotometer. Fluorescence spectra were recorded on a JASCO FP-6500 Spectrofluorometer. The wavelengths obtained by fluorescence spectrometer were converted to wavenumber by using the equation $I(\nu) = \lambda^2 I(\lambda)$.[1] Absolute Quantum Yields (Φ_{FL}) were measured by a Hamamatsu Photonics Quantaurus QY equipped with integral sphere. The measurement error of this instrument is ± 3% of obtained Φ_{FL} values. Fluorescence lifetimes were measured at the most intense peaks, i.e., the λ_{em} of the compound in each solvents, using a Hamamatsu Photonics OB 920 Fluorescence Lifetime Spectrometer equipped with LEDs lamp which possesses 343 nm of wavelength, 12.6 nm of bandwidth, and 725 ps of pulse width. All lifetime data were collected in the range of 0-50 ns with 1024 channels (i.e. time/channels = 48.8 ps).

Computational Methodology. The equilibrium structures of the compounds investigated in this work were fully optimized by using the ωB97X-D method with 6-31G(d,p) basis set,[2] which is suitable for dealing with excited states because this method includes both long-range correction and dispersion correction.[3] The Analytical frequencies were obtained to ensure that a local energy minimum has been located. Then, the singlet- and triplet-spin excited states for the minima have been calculated by time-dependent density functional theory (TD-DFT). All calculations were performed by using the Gaussian 09 program package[4] on the TSUBAME 2.0 supercomputer at Tokyo Institute of Technology.

Materials. Unless otherwise noted, all reagents and chemicals were used without further purification. *n*-Butyllithium and sodium *tert*-butoxide were obtained from TCI (Tokyo, Japan). Piperidine and $Pd(OAc)_2$ were prepared from Wako Pure Chem. (Tokyo, Japan). Spectrograde hexane, toluene, THF, chloroform, dichloromethane, DMF, ethanol, methanol, and 4Å molecular sieve were purchased from Nacalai Tasque (Kyoto, Japan). Ultrapure water with more than 18.2 MΩ·cm was supplied by the Milli-Q system (Merck Millipore) and was used as solvent while measuring optical property. Spectrograde acetonitrile was obtained from DOJINDO (Kumamoto, Japan). 1,6-dibromopyrene was taken from the stock previously we synthesized.[5]

Synthesis of 1-bromo-6-(piperidin-1-yl)pyrene (2)

1,6-Dibromopyrene (5.0 g, 8.3 mmol), sodium *tert*-butoxide (1.79 g, 18.4 mmol), $Pd(OAc)_2$ (0.14 g, 0.64 mmol), BINAP (1.25 g, 2.01 mmol) and toluene (50 mL) were placed in a 100-mL two-necked flask under nitrogen. After stirring for 15 minutes, the flask was heated to 100 °C. Piperidine (1.6 mL 15.8 mmol) was then added to the solution and the resulting mixture was stirred for 12 h. Subsequently, it was quenched with water to separate the formed organic layer. The organic layer was washed with brine and dried over $MgSO_4$. The solvent was removed *in vacuo* and the residue was subjected to silica column chromatography by chloroform/hexane = 1:1 to afford product **2** as yellow powder (2.7 g, 53%). ^{1}H NMR (300 MHz, $CDCl_3$) δ 8.41 (d, J = 9.3 Hz, 1H), 8.26 (d, J = 9.3 Hz, 1H), 8.17-8.10 (m, 2H), 8.04 (d, J = 9.3 Hz, 1H), 8.00-7.91 (m, 2H), 7.72 (d, J = 8.1 Hz, 1H), 3.19 (m, 4H), 1.92 (tt, J = 5.8 Hz, 5.2 Hz, 4H), 1.71 (m, 2H).

Synthesis of 1-hydroxycarbonyl-6-(piperidin-1-yl)pyrene (3)

1-Bromo-6-(piperidin-1-yl)pyrene (2.0 g, 5.5 mmol) and anhydrous THF (30 mL) were placed in a 100-mL two-necked flask under nitrogen. Then *n*-BuLi (2.6 mL, 6.7 mmol) was added to the solution at -78 °C, to lithiate **2**. After stirring for 30 minutes, CO_2 was bubbled into the solution three times using a balloon. The mixture was then allowed to be gradually warmed to r.t., and stirred for 12 h. Subsequently, the mixture was quenched with water and organic layer was extracted by EtOAc. The solvent was removed *in vacuo*. Then, the residue was solved in THF and reprecipitated into hexane

to afford yellow powder. (820 mg, 45 %). ^{1}H NMR (300 MHz, $CDCl_3$) δ 13.2 (s, 1H), 9.07 (d, *J* = 9.3 Hz, 1H), 8.54 (d, *J* = 8.1 Hz, 1H), 8.46 (d, *J* = 9.3Hz, 1H), 8.31 (d, *J* = 8.1Hz, 1H), 8.27-8.20 (m, 3H), 7.87 (d, *J* = 8.4 Hz, 1H), 3.19 (m, 4H), 1.92-1.85 (quint, *J* = 5.4 Hz, 4H), 1.68 (m, 2H)

Synthesis of ethyl 4-(6-(piperidin-1-yl)pyrene-1-carboxamido)butanoate (4)

Hydroxycarbonyl-6-(piperidin-1-yl)pyrene (0.72 g, 2.2 mmol), DCC (0.54 g, 2.6 mmol), ethyl 4-aminobutyrate hydrochloride (0.55 g, 3.3 mmol) and anhydrous THF (50 mL) were placed in a 100-mL two-necked flask under nitrogen and stirred at 0 °C at room temperature for 16 h. Then the mixture was filtered and the solvent was evaporated. The residue was subjected to silica column chromatography using ethyl chloroform/hexane = 1:1. Subsequently, the mixture was recrystallized from EtOAc/EtOH to obtain yellowish powder. (700 mg, 72 %). Mp 159.5-162.3 °C; ^{1}H NMR (300 MHz, $CDCl_3$) δ 8.47 (d, *J* = 9.3 Hz, 1H), 8.41 (d, *J* = 9.3 Hz, 1H), 8.14 (d, *J* = 8.1 Hz, 1H), 8.10-8.02 (m, 4H), 7.76 (d, *J* = 8.1Hz, 1H), 4.13 (q, *J* = 7.2 Hz, 2H), 3.71-3.64 (m, 2H), 3.22 (brs, 4H), 2.52 (t, *J* = 7.2 Hz, 2H), 2.07 (tt, *J* = 7.0 Hz, 7.1 Hz, 2H), 1.94 (m, 4H), 1.72 (brs, 2H), 1.24 (t, *J* = 7.2 Hz, 3H); ^{13}C NMR (100 MHz, $CDCl_3$) δ 173.8, 170.8, 150.3, 133.2, 130.7, 129.5, 129.1, 126.9, 126.6, 126.4, 126.1, 125.9, 125.2, 124.9, 124.0, 122.8, 117.9, 77.7, 61.0, 55.5, 40.1, 32.3, 27.1, 25.2, 25.0, 14.6; FT-IR (KBr) 1726 cm^{-1}, 1621 cm^{-1}; MS (FAB) Calcd for $C_{28}H_{30}N_2O_3$:442.2256, Found: 442.2256 ($[M]^+$).

Synthesis of 4-(6-(piperidin-1-yl)pyrene-1-carboxamido)butanoic acid (PSAC)

The mixture of compound **4** (200 mg, 0.45 mmol) and KOH aq. (25 mg, 0.45 mmol) in THF (20 mL) was stirred at room temperature for overnight. Then, pH was neutralized by dropping 2M HCl aq. The organic layer was extracted with ethylacetate and chloroform, and then was washed with brine. After the solvent was removed *in vacuo*, the residue was recrystalized from CH_2Cl_2 / Hexane to afford yellow powder. (36 mg, 19 %). Mp 216.0−217.5 °C; ^{1}H NMR (300 MHz, $CDCl_3$) δ 8.51 (d, *J* = 9.1 Hz, 1H), 8.41 (d, *J* = 9.2 Hz, 1H), 8.12 (d, *J* = 8.3 Hz, 4H), 8.08-8.00 (m, 4H), 7.75 (d, *J* = 8.2 Hz, 1H), 6.25 (m, 1H), 3.72-3.66 (m, 2H), 3.24-3.21 (m, 4H), 2.56 (t, *J* = 7.1 Hz, 2H), 2.08 (tt, *J* = 7.1 Hz, 6.7 Hz, 2H), 1.94 (tt, *J* = 5.6 Hz, 4.9 Hz, 4H), 1.76-1.69 (m, 2H) ; ^{13}C NMR (100 MHz, $CDCl_3$) δ 175.2, 170.0, 150.2, 132.6, 132.4, 129.1, 129.0, 127.2, 127.1, 126.9, 126.1, 125.9, 125.3, 124.8, 124.6, 124.5, 123.5, 118.6, 55.4, 39.6, 32.1, 27.1,

25.5, 24.9; FT-IR (KBr) 3326 cm^{-1}, 1626 cm^{-1}; MS (FAB) Calcd for $C_{26}H_{26}N_2O_3$:414.1943, Found: 414.1945 ($[M]^+$).

Synthesis of *N*-butylpyrene-6-(piperidin-1-yl)-1-carboxamide (PSA)

Compound **3** (0.17 g, 0.52 mmol), oxalyldichloride (0.45 mL, 5.2 mmol), 3 drops of DMF and 10 mL of CH_2Cl_2 were placed in a 50-mL two-necked flask under nitrogen and stirred for 3 hours to afford acid chloride. Subsequently excess oxalylchloride and solvent were removed *in vacuo*, then anhydrous CH_2Cl_2 (10 mL) were added again and the mixture was cooled to 0 °C. Next, triethyl amine (0.22 mL, 1.5 mmol), and *n*-butylamine (0.15mL, 1.5 mmol) was added to the mixture and was then allowed to be gradually warmed to room temperature. The mixture was stirred overnight. The organic layer was washed with brine. It was dried over $MgSO_4$ and then evaporated *in vacuo*. The residue was subjected to silica column chromatography using ethyl acetate/hexane = 1:5. Subsequent recrystallization from hexane afforded **PSA** as a yellow solid (40 mg, 20%). Mp 216.0−217.0 °C; ^{1}H NMR (400 MHz, $CDCl_3$) δ 8.46 (d, *J* = 9.4 Hz, 1H), 8.39 (d, *J* = 9.2 Hz, 1H), 8.13 (d, *J* = 8.1 Hz, 1H), 8.07-8.01 (m, 4H), 7.75 (d, *J* = 8.4Hz, 1H), 6.08 (t, *J* = 5.2 Hz, 1H), 3.64-3.59 (m, 2H), 3.21 (brs, 4H), 1.93 (tt, *J* = 5.4 Hz, 5.6 Hz, 4H), 1.73-1.66 (m, 2H), 1.49 (tq, *J* = 7.44 Hz, 7.44 Hz, 2H), 1.01 (t, *J* =7.4 Hz, 3H); ^{13}C NMR (100 MHz, $CDCl_3$) δ 214.5, 170.2, 149.9, 132.7, 130.8, 128.6, 126.5, 126.2, 126.0, 125.7, 124.9, 124.5,124.4, 123.6, 122.4, 117.5, 77.2, 76.9, 55.1, 49.9, 40.0, 31.8, 26.7, 24.5, 20.2, 13.8; FT-IR (KBr) 1617 cm^{-1}; MS (FAB) Calcd for $C_{26}H_{28}N_2O$: 384.2202, Found: 384.2206 ($[M]^+$).

Synthesis of *N,N*-Diethylpyrene-6-(piperidin-1-yl)-1-carboxamide (PTA)

1-Bromo-6-(piperidin-1-yl)pyrene (**2**) (0.3 g, 0.82 mmol) and anhydrous THF (10 mL) were placed in a 50-mL two-necked flask under nitrogen. Then *n*-BuLi (0.083 g, 0.99 mmol) was added to the solution at -78 °C, to lithiate **2**. After stirring for 30 minutes, *N,N*-diethylcarbomoyl chloride (0.13 mL, 0.99 mmol) was added into the solution. The mixture was then allowed to be gradually warmed to room temperature and stirred overnight. The reaction was quenched with small portion of water, then THF was removed *in vacuo*. To the residue chloroform was added and then the organic layer was washed with brine. The organic layer was dried over $MgSO_4$ and the solvent was

evaporated *in vacuo*. The residue was subjected to silica column chromatography using ethyl acetate/hexane = 1:5. Subsequent recrystallization in hexane and **PTA** was obtained (81 mg, 25%). Mp 157.8−159.4 °C; ^{1}H NMR (400 MHz, $CDCl_3$) δ 8.44 (d, *J* = 9.5 Hz, 1H), 8.13-8.11 (m, 2H), 8.05-8.00 (m, 2H), 7.88-7.84 (m, 2H), 7.74 (d, *J* = 8.3 Hz, 1H), 3.93-3.89 (m, 1H), 3.65-3.61 (m, 1H), 3.20-3.09 (m, 6H), 1.92 (tt, *J* = 5.3 Hz, 5.1Hz, 4H), 1.69 (m, 2H), 1.43 (t, *J* = 7.1 Hz, 3H), 0.97 (t, *J* = 7.1 Hz, 3H); ^{13}C-NMR (100 MHz, $CDCl_3$) δ 170.9, 150.1, 149.5, 131.6, 131.4, 128.5, 127.7, 126.1, 125.9, 125.8, 125.2, 124.9, 124.0, 123.9, 123.4, 122.0, 117.4, 64.4, 55.1, 50.7, 43.2, 39.2, 26.7, 24.5, 14.2, 13.6, 13.2 FT-IR (KBr) 1617 cm^{-1} MS (FAB) Calcd for $C_{26}H_{28}N_2O$: 384.2202, Found: 384.2211 ($[M]^+$). Anal. Calcd for $C_{26}H_{28}N_2O$: C, 81.21; H, 7.34; N, 7.29. Found: C, 80.86; H, 7.30; N, 7.16.

B. ^{1}H and ^{13}C NMR Spectra

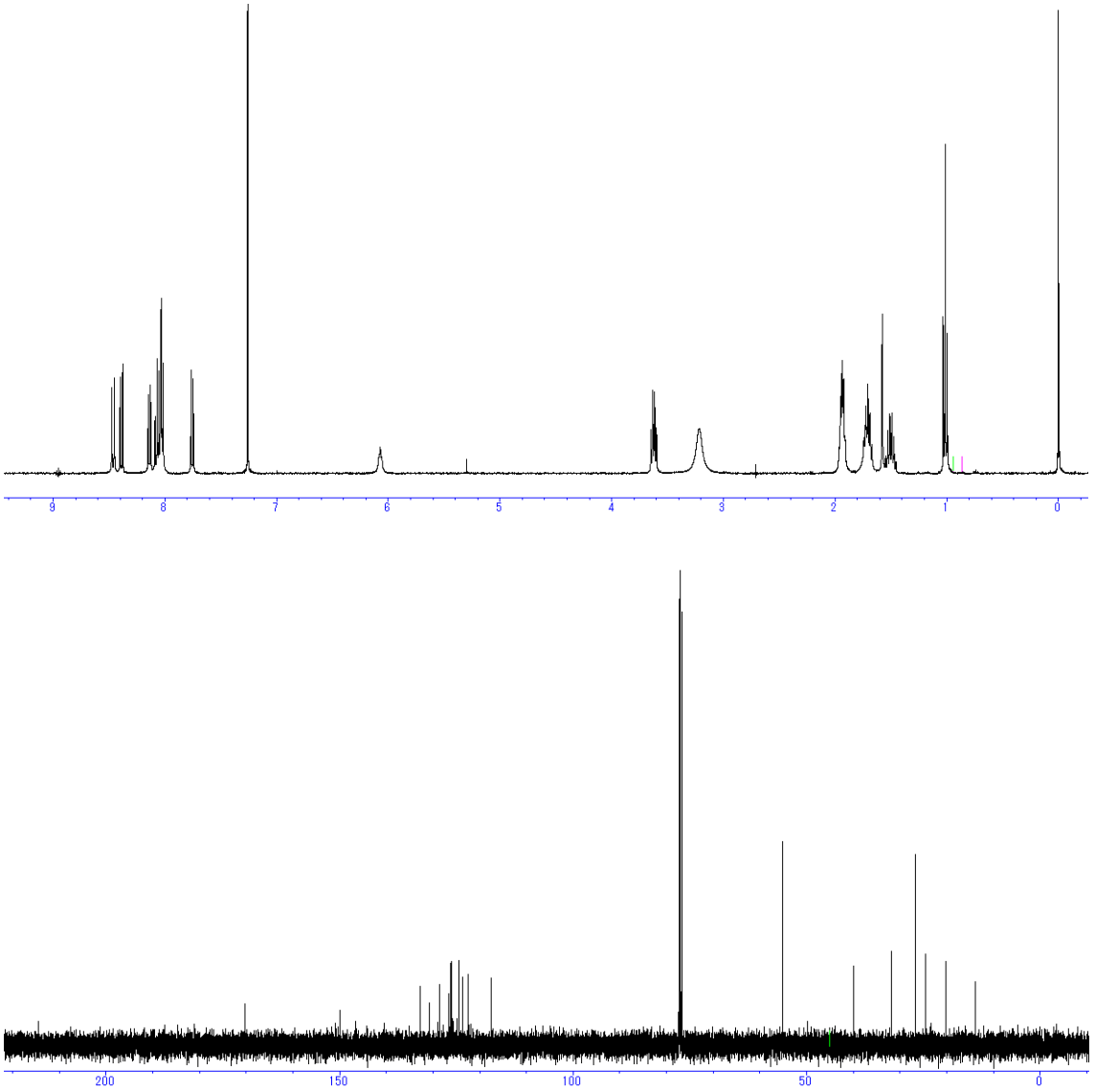

Fig. S1 ^{1}H and ^{13}C NMR spectra of **PSA** ($CDCl_3$, r.t.).

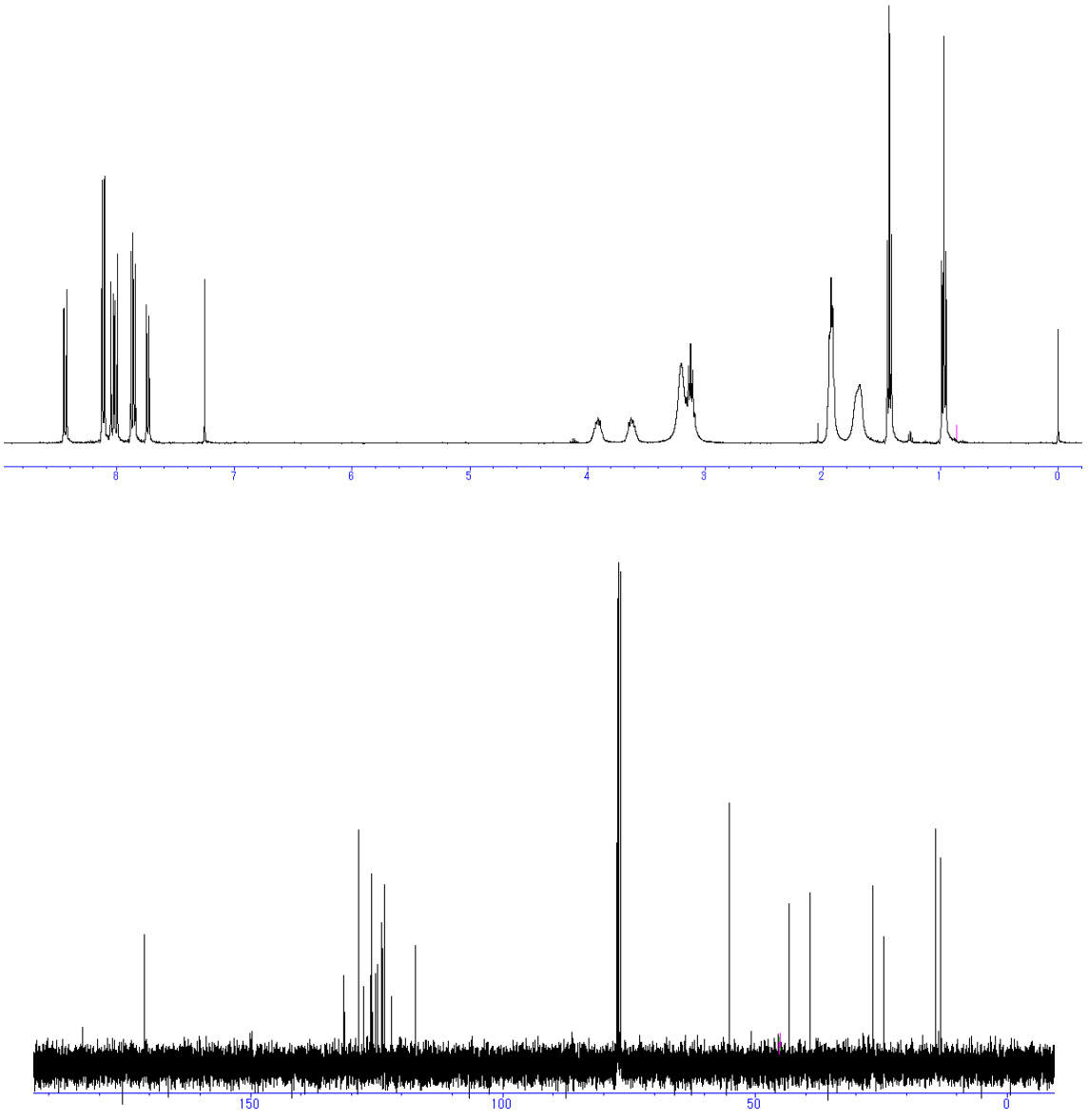

Fig. S2 ^{1}H and ^{13}C NMR spectra of **PTA** ($CDCl_3$, r.t.).

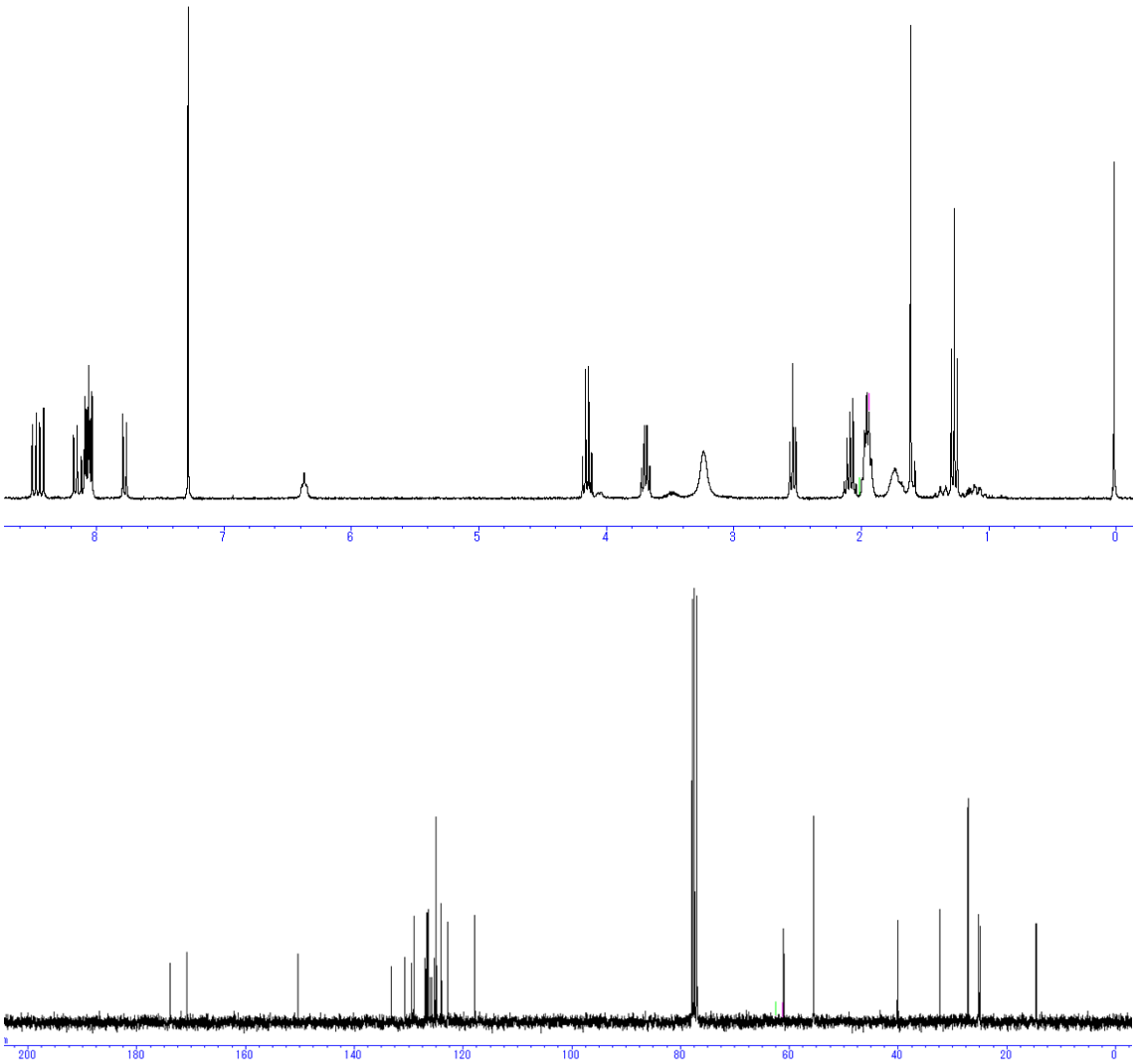

Fig. S3 ^{1}H and ^{13}C NMR spectra of compound **4** ($CDCl_3$, r.t.).

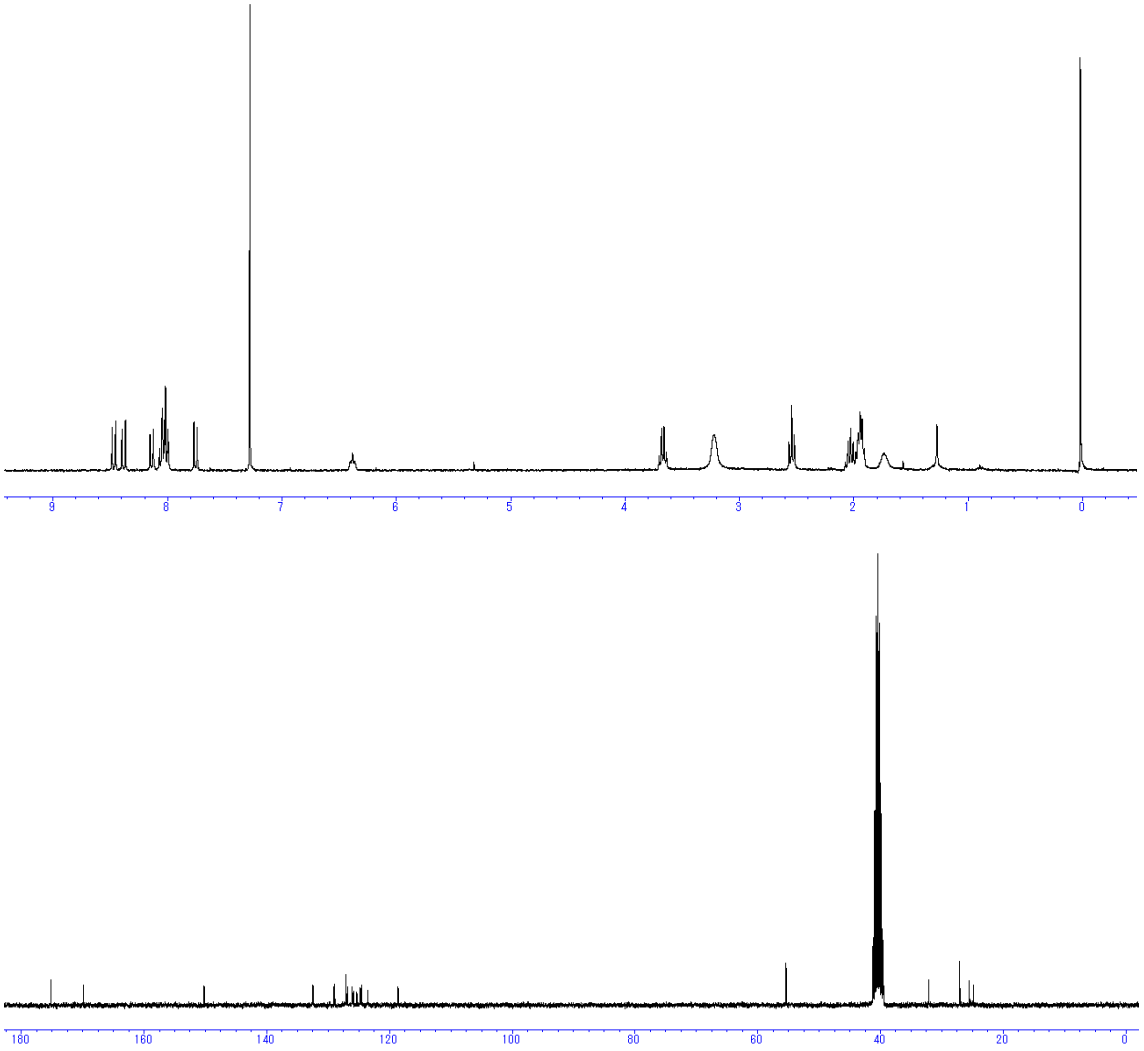

Fig. S4 ^{1}H NMR spectra ($CDCl_3$, 50 ^{o}C) and 13C NMR spectra (DMSO, r.t.) of **PSAC**.

C. Examination of water solubility of PSAC

PSAC was dissolved in THF to prepare the stock solution (10^{-3} μM). To the H_2O in 10 mL of measuring flask was added small amount of stock solution to afford the diluted **PSAC** water solution in the range between 1~10 μM. In this region, fluorescence intensities of **PSAC** were proportional to the dye concentration, and the measured Φ_{FL} of **PSAC** in 5 μM was 97 %, indicating **PSAC** was not precipitated and soluble in this range where the measurement of fluorescence properties can be carried out correctly.

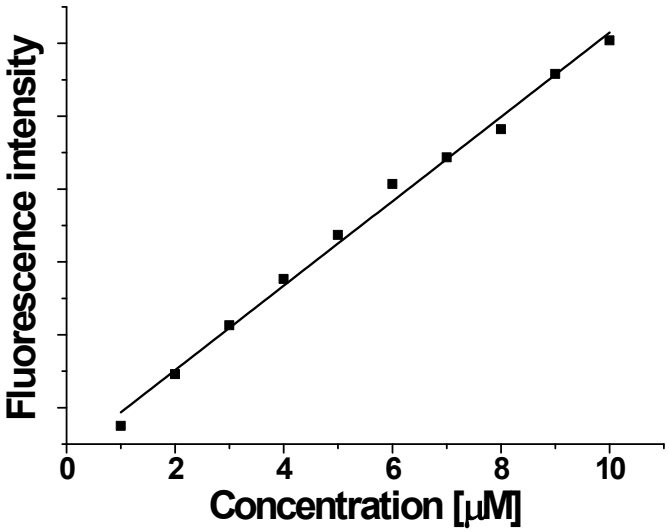

Fig. S5 Plots of fluorescence intensity of **PSAC** monitored at 539 nm against dye concentration in H_2O ($r^2 = 0.99$).

D. Detailed photophysical data of PSA and PTA

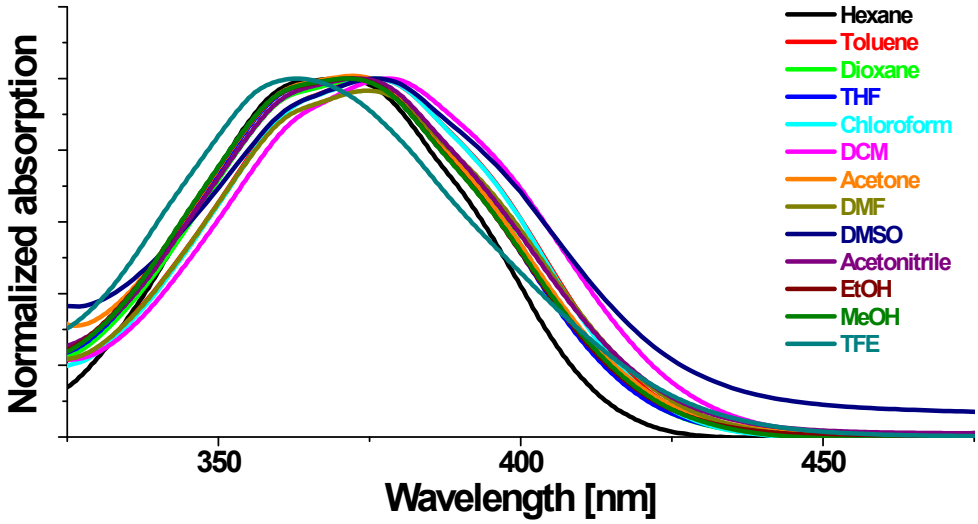

Fig. S6 Normalized absorption spectra of **PSA** in solvents of different polarities (room temperature).

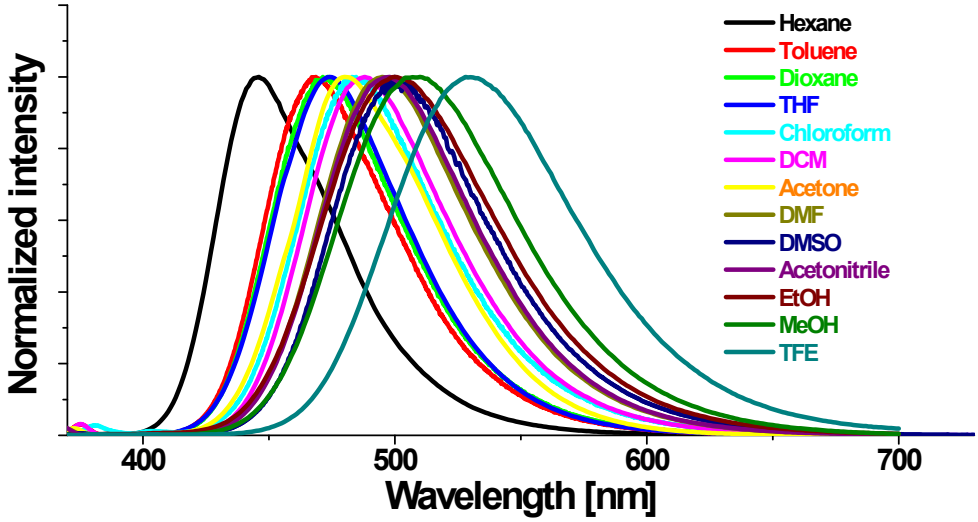

Fig. S7 Normalized fluorescence spectra of **PSA** in solvents of different polarities (λ_{ex} = $\lambda_{abs,\ max}$, Optical Density (O.D.) = 0.1, room temperature).

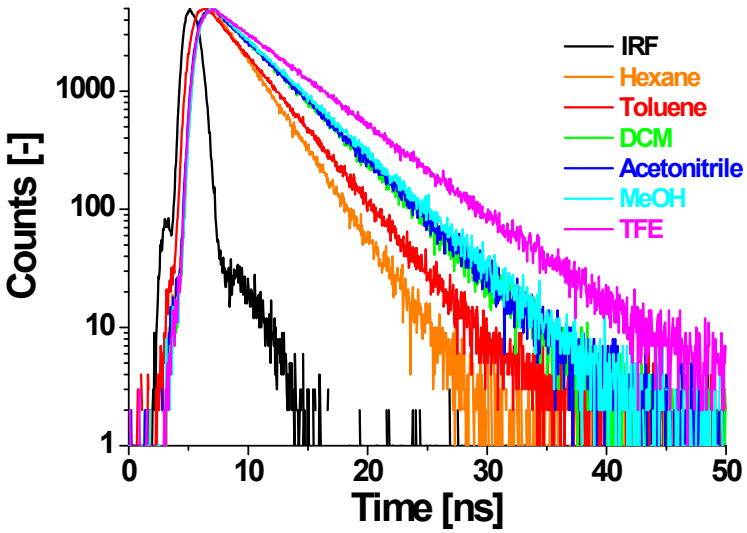

Fig. S8 Fluorescence decay profiles for **PSA** in several solvents of different polarities (λ_{ex} = 343 nm, monitored at $\lambda_{em,\ max}$, 5000 counts).

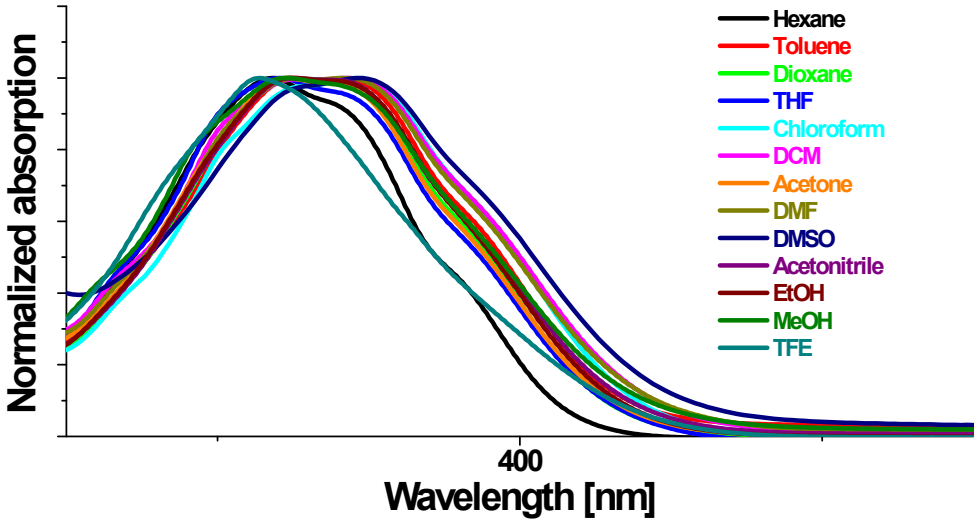

Fig. S9 Normalized absorption spectra of **PTA** in solvents of different polarities (room temperature).

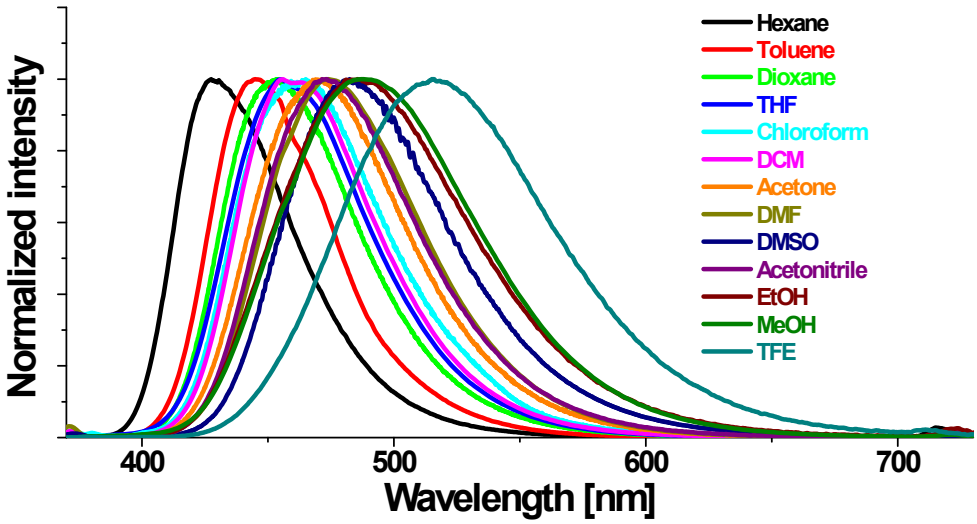

Fig. S10 Normalized fluorescence spectra of **PTA** in organic solvents of different polarities ($\lambda_{ex} = \lambda_{abs,\,max}$, Optical Density (O.D.) = 0.1, room temperature).

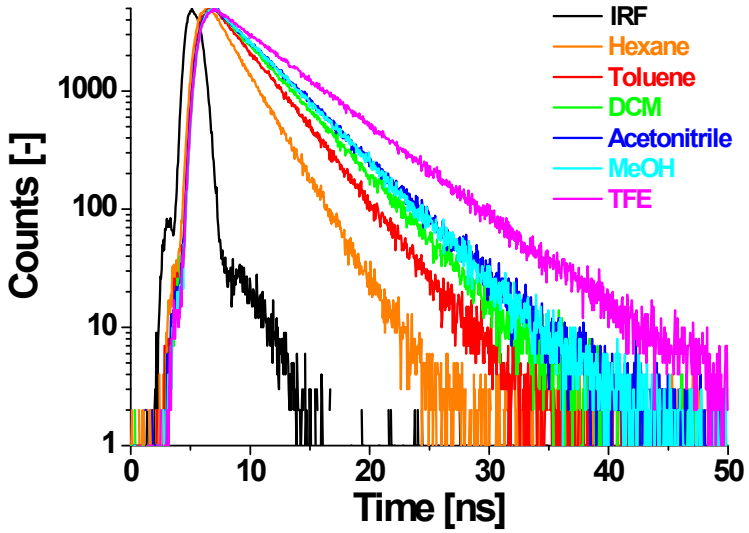

Fig. S11 Fluorescence decay profiles for **PTA** in several solvents of different polarities (λ_{ex} = 343 nm, monitored at $\lambda_{em,\,max}$, 5000 counts).

Table S1. Spectroscopic parameter of **PSA** and **PTA** in organic solvents with different polarities.

Solvent	Δf	$\lambda_{abs,\ max}$ [nm]		$\lambda_{em,\ max}$ [nm]		Φ_{FL} [%]		τ [ns]		k_f^* [10^7 s^{-1}]		k_{nr}^* [10^7 s-1]	
		PSA	**PTA**	**PSA**	**PTA**	**PSA**	**PTA**	**PSA**	**PTA**	**PSA**	**PTA**	**PSA**	**PTA**
Hexane	0.000	371	359	446	428	97	66	2.8	2.4	0.346	0.275	0.011	0.142
Toluene	0.013	376	363	469	446	95	85	3.5	3.4	0.275	0.252	0.014	0.045
Dioxane	0.020	373	362	471	454	95	92	4.2	3.9	0.225	0.237	0.012	0.021
THF	0.210	372	360	474	455	94	81	3.7	4.0	0.258	0.203	0.016	0.048
Chloroform	0.148	376	373	485	465	91	52	3.9	3.4	0.236	0.153	0.023	0.142
DCM	0.217	378	372	488	456	99	83	4.2	3.9	0.236	0.215	0.002	0.044
Acetone	0.284	372	361	480	471	93	94	3.9	4.0	0.237	0.235	0.018	0.015
DMF	0.274	375	371	495	474	93	83	4.5	4.2	0.206	0.200	0.016	0.041
DMSO	0.263	376	374	500	482	88	85	4.5	4.5	0.196	0.190	0.027	0.034
Acetonitrile	0.305	373	363	498	472	95	89	4.3	4.3	0.221	0.206	0.012	0.026
Ethanol	0.289	372	362	500	485	99	91	4.2	4.5	0.235	0.202	0.002	0.020
Methanol	0.309	372	362	510	487	93	83	4.5	4.2	0.209	0.198	0.016	0.040
TFE	0.280	363	357	528	516	98	97	5.6	5.6	0.174	0.173	0.004	0.005

*k_f and k_{nr}: the rate constanst of radiative and nonradiative decay, respectively. Assuming a single emission state, k_f and k_{nr} are defined as follow; $k_f = \Phi_{FL} / \tau$, $k_{nr} = (1-\Phi_{FL}) / \tau$

E. Detailed photophysical data of PSAC

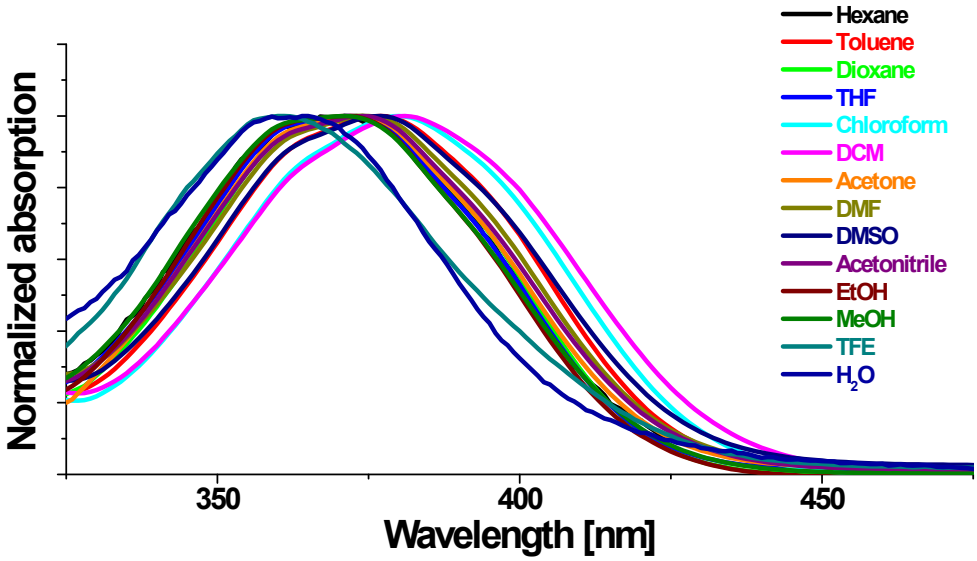

Fig. S12 Normalized absorption spectra of **PSAC** in solvents of different polarities (room temperature).

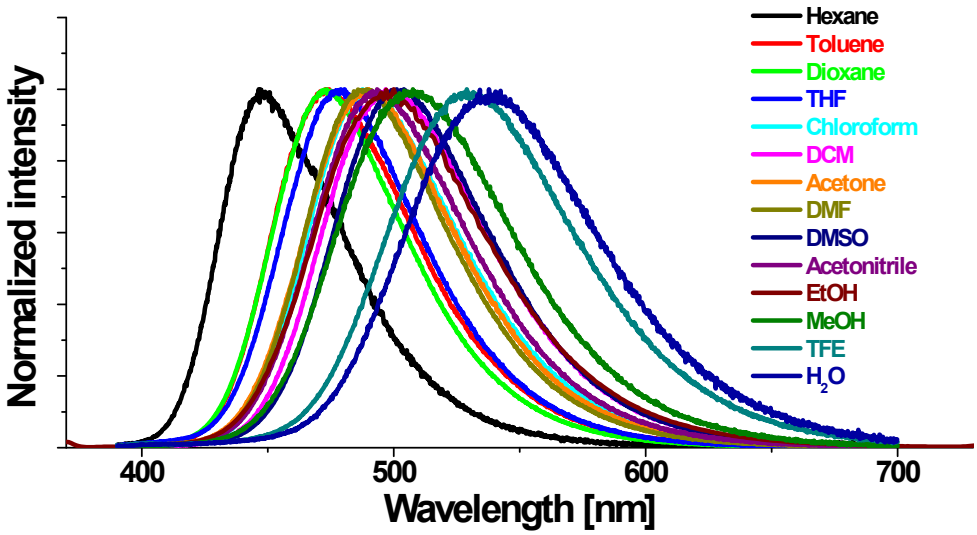

Fig. S13 Normalized fluorescence spectra of **PSAC** in organic solvents of different polarities ($\lambda_{ex} = \lambda_{abs,\ max}$, Optical Density (O.D.) = 0.1, room temperature).

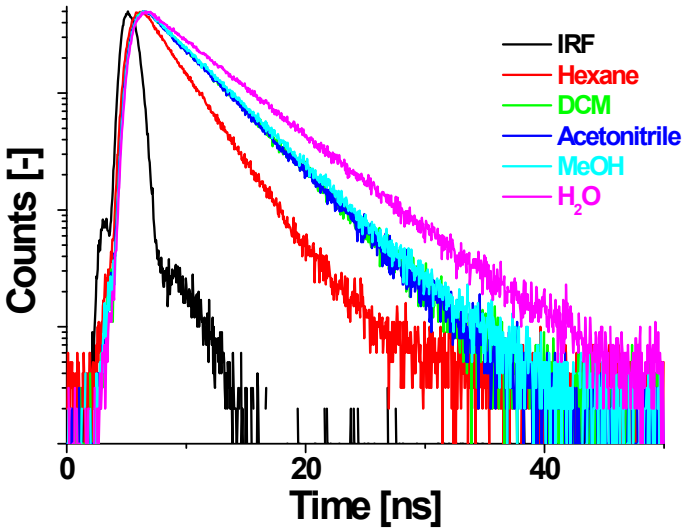

Fig. S14 Fluorescence decay profiles for **PSAC** in several solvents of different polarities (λ_{ex} = 343 nm, monitored at $\lambda_{em,\,max}$, 5000 counts).

Table S2. Spectroscopic parameter of **PSAC** in several solvents with different polarities.

Solvent	Δf	$\lambda_{abs,\,max}$ [nm]	$\lambda_{em,\,max}$ [nm]	Φ_{FL} [%]	τ [ns]	k_f [10^7 s^{-1}]	k_{nr} [10^7 s^{-1}]
Hexane*	0.000	371	446	-	-	-	-
Toluene	0.013	377	473	>99	3.2	0.307	0.0031
Dioxane	0.020	373	473	>99	3.9	0.252	0.0025
THF	0.210	372	480	>99	3.9	0.253	0.0026
Chloroform	0.148	380	488	>99	3.7	0.265	0.0027
DCM	0.217	381	497	>99	4.1	0.241	0.0024
Acetone	0.284	373	490	99	3.9	0.257	0.0026
DMF	0.274	374	489	98	4.2	0.236	0.0048
DMSO	0.263	377	501	96	4.4	0.217	0.009
Acetonitrile	0.305	374	493	>99	4.1	0.243	0.0025
EtOH	0.289	372	500	98	4.5	0.216	0.0044
MeOH	0.309	371	508	>99	4.2	0.233	0.0024
TFE	0.280	360	529	>99	5.3	0.189	0.0019
H_2O	0.320	360	538	97	5.3	0.182	0.0056

*Hexane: The Φ_{FL} value of **PSAC** in hexane was not obtained because of low solubility that induced the precipitation of **PSAC** before the measurement.

F. Lippert Mataga plots

The change in dipole moment (μ_e–μ_g) for **PSA**, **PTA** and **PSAC** were estimated by plotting the Lippert equation defined as below:

$(\nu_{abs} - \nu_{fl}) = 2(\mu_e-\mu_g)^2\Delta f / hca^3$, $\Delta f = (\varepsilon - 1)/(2\varepsilon + 1) - (n^2 - 1)/(2n^2 + 1)$

In this equation, ν_{abs} and ν_{fl} are the wavenumbers of the absorption and fluorescence; μ_e and μ_g are the excited and ground state dipole moments; c is the speed of light; h is Planck's constant; a is the radius of the cavity; n and ε are the refractive index and dielectric constant, respectively; the orientation polarizability function were calculated by using known values of n and ε. The cavity radius for all compounds a were taken as 4.82 based on optimized structures in the ground states caluclated by DFT (wB97X-D/6-31G(d,p)). The data in hydrogen-bonding donor solvents were excluded to avoid specific effect between solute-solvent interactions.

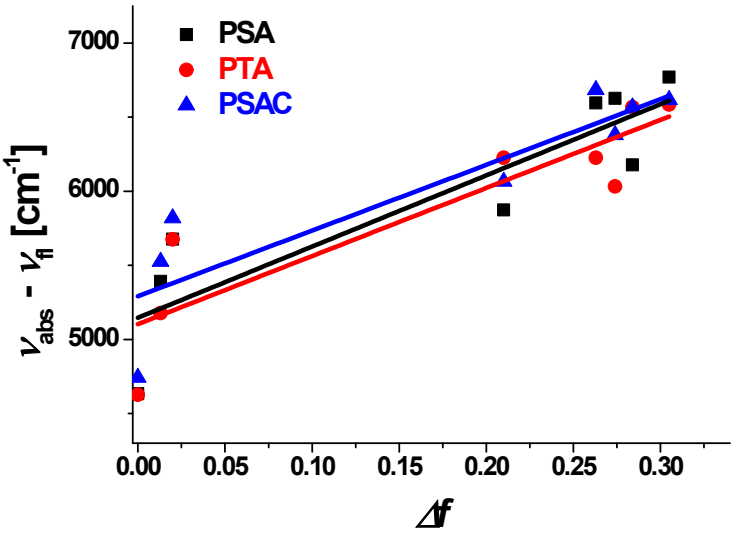

Fig. S15 Stokes shifts (ν_{abs} - ν_{fl}) of **PSA**, **PTA** and **PSAC** vs the orientation polarizability function (Δf) (Lippert-Mataga plot). The results of the linear least-squares fit: ν_{abs} - ν_{fl} = 5146.2 + 4802.9Δf (r^2 = 0.80) for **PSA**, 5103.3 + 4593.3Δf (r^2 = 0.81) for **PTA**, and 5291.4 + 4432.4Δf (r^2 = 0.80) for **PSAC**.

G. Fluorescence behavior of PA in the presence of H_2O

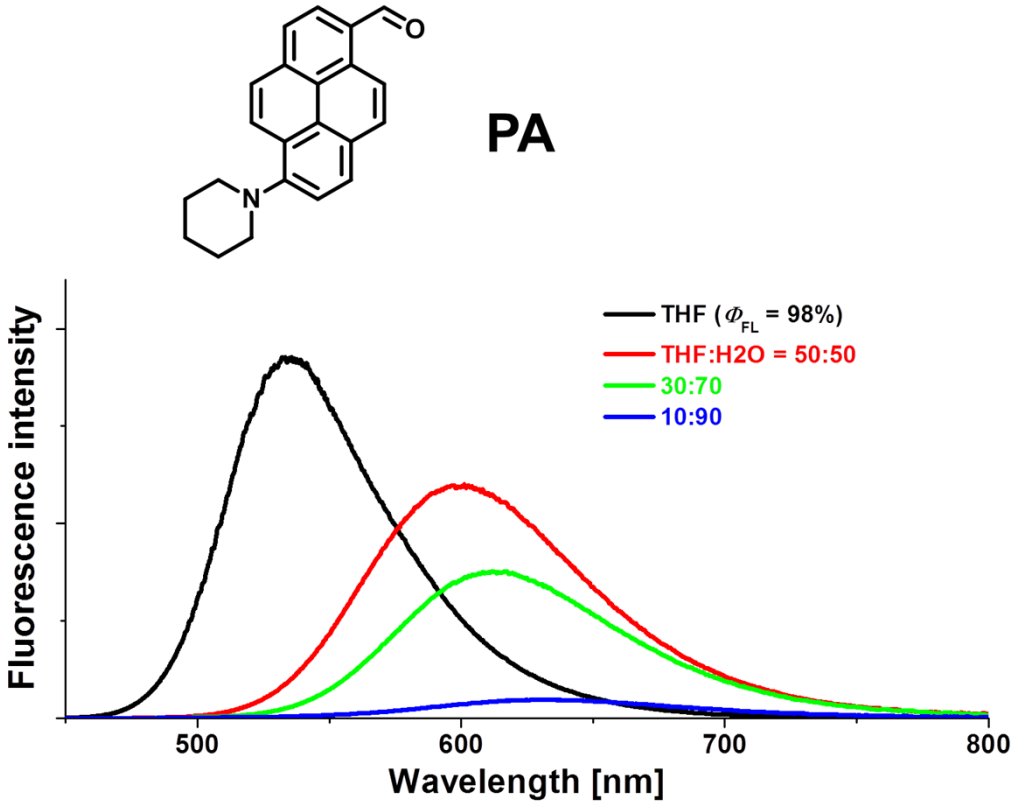

Fig. S16 Fluorescence spectra of **PA** in the mixture of THF and H_2O ($\lambda_{ex} = \lambda_{abs,\ max}$, dye concentration: 2.5×10^{-6} M, room temperature).

H. DFT/TDDFT calculations

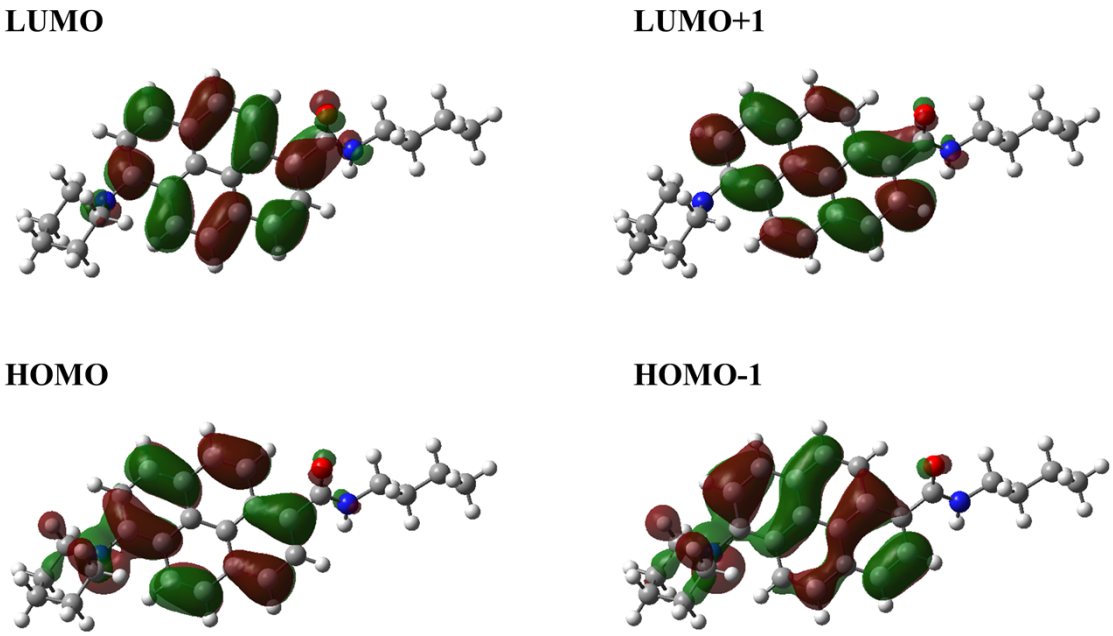

Fig. S17 The MOs of **PSA** calculated by DFT (ωB97X-D/6-31G(d,p)).

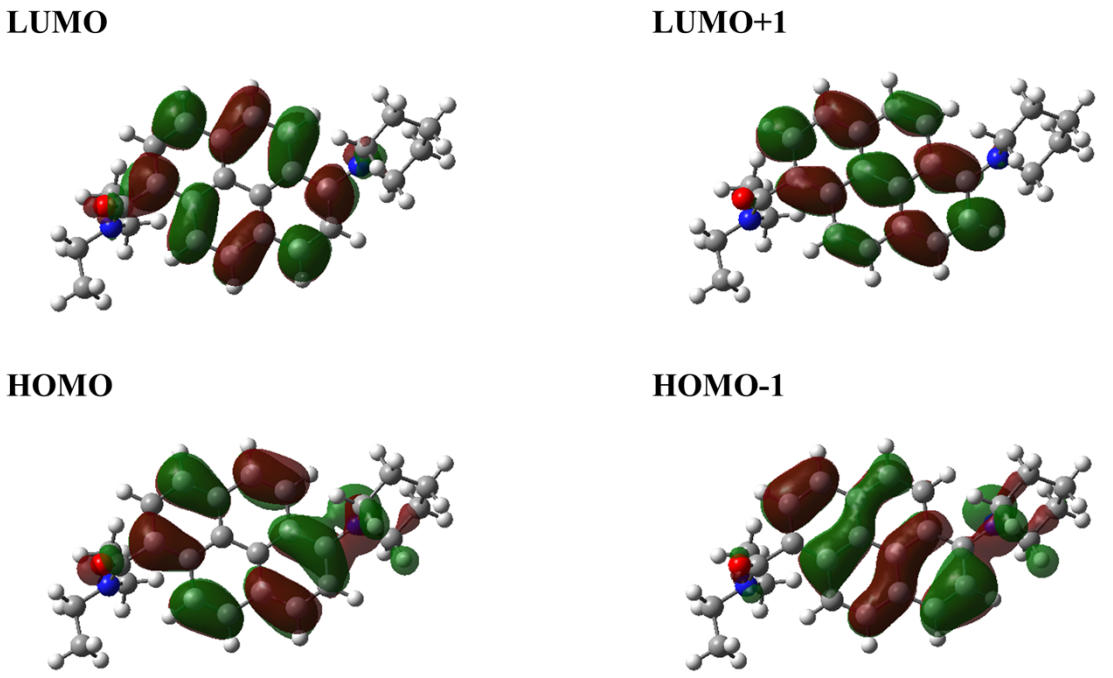

Fig. S18 The MOs of **PTA** calculated by DFT (ωB97X-D/6-31G(d,p)).

Table S3. Excitation energy, osillator strength, main transition orbital, and their calculated for **PSA** and **PTA** using TD-DFT (ωB97X-D/6-31G(d,p))

	State	Excitation energy [eV]	Oscillator strength	Main transition orbital	Contribution
PSA	T1	1.98		HOMO → LUMO	0.84
	T2	3.57		HOMO → LUMO+1	1
	T3	3.63		HOMO-5 → LUMO	0.29
				HOMO-3 → LUMO	0.17
				HOMO → LUMO+2	0.48
	T4	3.68		HOMO-6 → LUMO	0.17
				HOMO-1 → LUMO	0.49
				HOMO → LUMO+3	0.31
	S1	3.69	0.5523	HOMO → LUMO	0.97
	T5	3.82		HOMO-2 → LUMO	0.43
				HOMO-1 → LUMO	0.41
				HOMO → LUMO+3	0.1
	S2	3.93	0.0109	HOMO-1 → LUMO	0.3
				HOMO → LUMO+1	0.61
	T6	4.08		HOMO-2 → LUMO+1	0.21
				HOMO-1 → LUMO+1	0.7
PTA	T1	2		HOMO → LUMO	0.82
	T2	3.59		HOMO → LUMO+1	0.9
	T3	3.64		HOMO-5 → LUMO	0.39
				HOMO → LUMO+1	0.11
				HOMO → LUMO+2	0.47
	T4	3.73		HOMO-6 → LUMO	0.2
				HOMO-2 → LUMO	0.12
				HOMO-1 → LUMO	0.34
				HOMO → LUMO+3	0.34
	S1	3.75	0.4985	HOMO → LUMO	0.95
	T5	3.84		HOMO-2 → LUMO	0.28
				HOMO-1 → LUMO	0.59
	S2	3.96	0.0301	HOMO-1 → LUMO	0.3
				HOMO → LUMO+1	0.62
	T6	4.08		HOMO-1 → LUMO+1	0.74

Table S4. Atom coordinates and absolte energies of **PSA** and **PTA** in theoretical calculations.

PSA (ground): E(RwB97XD) = -1192.0612517 A.U.

Center number	Atomic number	Coordinate (Angstroms)		
		X	Y	Z
1	6	2.382305	-1.701537	-0.244465
2	6	1.15418	-2.336783	-0.317539
3	6	-0.029017	-1.595109	-0.274021
4	6	0.042634	-0.183095	-0.135496
5	6	1.306874	0.467977	-0.049065
6	6	2.477879	-0.313701	-0.118512
7	6	-1.318301	-2.220241	-0.389676

8	6	-1.166962	0.581312	-0.083617
9	6	-2.426601	-0.069144	-0.151279
10	6	-2.458677	-1.49469	-0.337775
11	6	-3.612096	0.693335	-0.05803
12	6	-3.522092	2.084383	0.025151
13	6	-2.290491	2.722694	0.05535
14	6	-1.100529	1.994253	0.024047
15	6	0.188323	2.623329	0.099193
16	6	1.333917	1.905299	0.073473
17	1	2.294804	2.394322	0.164801
18	1	0.226971	3.705402	0.189376
19	1	-1.356375	-3.295179	-0.541625
20	1	3.290912	-2.296656	-0.256159
21	1	1.103502	-3.417904	-0.407105
22	1	-3.425834	-1.967719	-0.466914
23	1	-4.427281	2.678332	0.087019
24	1	-2.247129	3.805716	0.129772
25	6	-5.173027	-0.642693	1.222679
26	6	-6.002106	0.739463	-0.581062
27	6	-6.300095	-1.653645	1.035844
28	1	-5.47001	0.110421	1.97681
29	1	-4.273988	-1.135925	1.599089
30	6	-7.152322	-0.229296	-0.848935
31	1	-6.353571	1.521475	0.11977
32	1	-5.698598	1.238324	-1.505765
33	6	-7.532932	-0.983964	0.426091
34	1	-6.543669	-2.110394	2.000765
35	1	-5.949031	-2.453468	0.372261
36	1	-8.011321	0.325347	-1.240903
37	1	-6.836855	-0.940843	-1.620707
38	1	-8.312006	-1.724266	0.218468
39	1	-7.952427	-0.274472	1.15236
40	7	-4.855553	0.01385	-0.050193
41	6	3.843079	0.311944	-0.036758
42	8	4.139104	1.192091	0.761805
43	7	4.748388	-0.185435	-0.925746
44	1	4.441611	-0.854841	-1.611303
45	6	6.129919	0.257943	-0.92472
46	1	6.530931	0.122788	-1.934581
47	1	6.134543	1.329319	-0.702439
48	6	6.992312	-0.481004	0.098211
49	1	6.962567	-1.558267	-0.111758
50	1	6.54663	-0.33492	1.088577
51	6	8.439954	0.007019	0.102498
52	1	8.455603	1.084413	0.309013
53	1	8.872324	-0.120632	-0.898708
54	6	9.30416	-0.722228	1.128772
55	1	9.329293	-1.798418	0.927459
56	1	10.334326	-0.355174	1.116929

57	1	8.909665	-0.583331	2.140482

PTA (ground): E(RwB97XD) = -1192.0566963 A.U.

Center number	Atomic number	Coordinate (Angstroms)		
		X	Y	Z
1	6	-2.594227	-2.296203	-0.405813
2	6	-1.313265	-2.786957	-0.208128
3	6	-0.224574	-1.915234	-0.106777
4	6	-0.445438	-0.517207	-0.215458
5	6	-1.76338	-0.017152	-0.403154
6	6	-2.831689	-0.925231	-0.481782
7	6	1.113217	-2.387574	0.126138
8	6	0.660324	0.387123	-0.131987
9	6	1.975736	-0.113569	0.04546
10	6	2.158477	-1.531888	0.20382
11	6	3.063777	0.787178	0.08726
12	6	2.814312	2.159787	0.026028
13	6	1.523193	2.650289	-0.111433
14	6	0.432689	1.786164	-0.213696
15	6	-0.911032	2.262741	-0.399085
16	6	-1.955523	1.409513	-0.496203
17	1	-2.960729	1.790682	-0.646218
18	1	-1.071333	3.33499	-0.469385
19	1	1.26622	-3.455029	0.257263
20	1	-3.430564	-2.981204	-0.504361
21	1	-1.146122	-3.857576	-0.134686
22	1	3.157774	-1.893529	0.418906
23	1	3.642991	2.858034	0.066601
24	1	1.358038	3.722771	-0.165615
25	6	4.888784	-0.319244	-1.056099
26	6	5.370434	1.100971	0.842033
27	6	6.105182	-1.195964	-0.775303
28	1	5.164935	0.484059	-1.764892
29	1	4.095405	-0.903701	-1.527269
30	6	6.597035	0.2666	1.206095
31	1	5.691302	1.937907	0.191784
32	1	4.922732	1.534912	1.740572
33	6	7.185258	-0.403257	-0.037037
34	1	6.492636	-1.594459	-1.718712
35	1	5.79012	-2.049257	-0.162228
36	1	7.342233	0.907134	1.689349
37	1	6.296177	-0.497841	1.931716
38	1	8.023572	-1.052445	0.234711
39	1	7.584795	0.369962	-0.70737
40	7	4.37479	0.260925	0.189588
41	6	-4.244598	-0.469614	-0.747426
42	8	-4.756408	-0.654603	-1.844133
43	7	-4.915227	0.134513	0.277517
44	6	-6.283983	0.57347	0.025487

45	1	-6.724142	-0.102166	-0.710051
46	1	-6.848072	0.47489	0.958671
47	6	-6.334609	2.009227	-0.487762
48	1	-5.805351	2.078248	-1.441532
49	1	-5.867449	2.698846	0.222924
50	1	-7.369002	2.329082	-0.644003
51	6	-4.409586	0.239386	1.641787
52	1	-4.835933	1.148936	2.078189
53	1	-3.328895	0.384564	1.620819
54	6	-4.757052	-0.977055	2.495633
55	1	-4.408131	-0.837656	3.522917
56	1	-5.837635	-1.147417	2.521488
57	1	-4.278028	-1.871771	2.088161

I. Supplementary references

[1] J. R. Lakowicz, *Principles of Fluorescence Spectroscopy Third Edition*, Springer+Business Media, LLC; New York, 2006.

[2] a) J.-D. Chai, M. Head-Gordon, *Phys. Chem. Chem. Phys.* **2008**, *10*, 6615-6620; b) R. Ditchfield, W. J. Hehre, J. A. Pople, *J. Chem. Phys.* **1971**, *54*, 724-728; c) W. J. Hehre, R. Ditchfield, J. A. Pople, *J. Chem. Phys.* **1972**, *56*, 2257-2261; d) P. C. Hariharan, J. A. Pople, *Theor. Chem. Acc.* **1973**, *28*, 213-222: e) P. C. Hariharan, J. A. Pople, *Mol. Phys.* **1974**, *27*, 209-214.

[3] a) N. Mardirossian, J. A. Parkhill, M. Head-Gordon, *Phys. Chem. Chem. Phys.* **2011**, *13*, 19325-19337; b) D. Jacquemin, E. A. Perpète, I. Ciofini, C. Adamo, *Theor. Chem. Acc.* **2011**, *128*, 127-136.

[4] Gaussian 09, Revision C.01, M. J. Frisch, G. W. Trucks, H. B. Schlegel, G. E. Scuseria, M. A. Robb, J. R. Cheeseman, G. Scalmani, V. Barone, B. Mennucci, G. A. Petersson, H. Nakatsuji, M. Caricato, X. Li, H. P. Hratchian, A. F. Izmaylov, J. Bloino, G. Zheng, J. L. Sonnenberg, M. Hada, M. Ehara, K. Toyota, R. Fukuda, J. Hasegawa, M. Ishida, T. Nakajima, Y. Honda, O. Kitao, H. Nakai, T. Vreven, J. A. Montgomery, Jr., J. E. Peralta, F. Ogliaro, M. Bearpark, J. J. Heyd, E. Brothers, K. N. Kudin, V. N. Staroverov, R. Kobayashi, J. Normand, K. Raghavachari, A. Rendell, J. C. Burant, S. S. Iyengar, J. Tomasi, M. Cossi, N. Rega, J. M. Millam, M. Klene, J. E. Knox, J. B. Cross, V. Bakken, C. Adamo, J. Jaramillo, R. Gomperts, R. E. Stratmann, O. Yazyev, A. J. Austin, R. Cammi, C. Pomelli, J. W. Ochterski, R. L. Martin, K. Morokuma, V. G. Zakrzewski, G. A. Voth, P. Salvador, J. J. Dannenberg, S. Dapprich, A. D. Daniels, Ö. Farkas, J. B. Foresman, J. V. Ortiz, J. Cioslowski, and D. J. Fox, Gaussian, Inc., Wallingford CT, 2010.